MASSACHUSETTS INSTITUTE OF TECHNOLOGY

Ocean Engineering

Cambridge, Massachusetts 02139

MASSACHUSETTS INSTITUTE OF TECHNOLOGY
Department of Ocean Engineering
Cambridge, MA 02139

REVIEW, FINAL REPORT

A DEFORMED WAKE MODEL FOR MARINE PROPELLERS

by

J. E. Kerwin

October, 1976

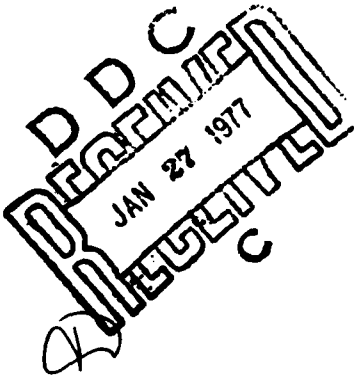

This research was carried out under the
Naval Sea Systems Command
General Hydromechanics Research Program
Subproject SR 009 01 01, Administered by the
Naval Ship Research and Development Center
Office of Naval Research Contract ~~N0014~~-67-A-0204-0059
MIT OSP N00014-

SECURITY CLASSIFICATION OF THIS PAGE *(When Data Entered)*

REPORT DOCUMENTATION PAGE

READ INSTRUCTIONS BEFORE COMPLETING FORM

1. REPORT NUMBER [redacted]
2. GOVT ACCESSION NO.
3. RECIPIENT'S CATALOG NUMBER

(6) 4. TITLE *(and Subtitle)*
A DEFORMED WAKE MODEL FOR MARINE PROPELLERS.

(9) 5. TYPE OF REPORT & PERIOD COVERED
Final Report.

6. PERFORMING ORG. REPORT NUMBER

(10) 7. AUTHOR(s)
Justin E. Kerwin

(15) 8. CONTRACT OR GRANT NUMBER(s)
N00014 67-A-0204-0059
Nour

9. PERFORMING ORGANIZATION NAME AND ADDRESS
Depart. of Ocean Engineering
M.I.T., Cambridge, MA 02139

10. PROGRAM ELEMENT, PROJECT, TASK AREA & WORK UNIT NUMBERS
SR009-01-01

11. CONTROLLING OFFICE NAME AND ADDRESS
Office of Naval Research

(11) 12. REPORT DATE
Nov[redacted] 1976

13. NUMBER OF PAGES

14. MONITORING AGENCY NAME & ADDRESS *(if different from Controlling Office)*
David Taylor Naval Research and Development Center, Bethesda, MD 20084

15. SECURITY CLASS. *(of this report)*
Unclassified

15a. DECLASSIFICATION/DOWNGRADING SCHEDULE

16. DISTRIBUTION STATEMENT *(of this Report)*
Approved for public release; distribution unlimited

(12) 44 p.

17. DISTRIBUTION STATEMENT *(of the abstract entered in Block 20, if different from Report)*

(16) SR00701 (17) SR0099101

18. SUPPLEMENTARY NOTES
Sponsored by the Naval Sea Systems Command General Hydromechanics Research Program administered by the Naval Ship Research and Development Center

19. KEY WORDS *(Continue on reverse side if necessary and identify by block number)*
Propeller Theory
Vortex Wakes

20. ABSTRACT *(Continue on reverse side if necessary and identify by block number)*
Results are given of a systematic series of experiments in which the radius and pitch of propeller tip vorticies are measured and analyzed. The measurements of ultimate wake pitch are compared with theoretical predictions based both on a simple activator disc model and on a direct calculation of the self-induced velocities of the helical vortices. The effect of wake deformation on the computed radial distribution of pitch and camber is given for a specific design example.

DD FORM 1 JAN 73 1473 EDITION OF 1 NOV 65 IS OBSOLETE
S/N 0102-014-6601

406856

SECURITY CLASSIFICATION OF THIS PAGE *(When Data Entered)*

ABSTRACT

Results are given of a systematic series of experiments in which the radius and pitch of propeller tip vortices are measured and analyzed. The measurements of ultimate wake pitch are compared with theoretical predictions based both on a simple actvator disc model and on a direct calculation of the self-induced velocities of the helical vortices. The effect of wake deformation on the computed radial distribution of pitch and camber is given for a specific design example.

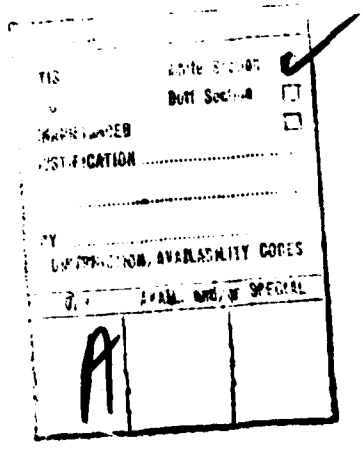

NOMENCLATURE

C_T = propeller thrust coefficient $\frac{T}{\frac{1}{2}\rho V_A^2 \pi R^2}$

D = propeller diameter

f_o/c = blade section camber/chord ratio

J = advance coefficient $\frac{V_A}{nD}$

K = number of propeller blades

K_Q = torque coefficient $\frac{Q}{\rho n^2 D^5}$

K_T = thrust coefficient $\frac{T}{\rho n^2 D^4}$

n = propeller rotational speed in revolutions/second

P = blade section pitch

P_i = pitch of trailing vortex sheet

P_o = pitch of trailing vortex sheet according to lifting line theory

P_w = pitch of trailing vortex in ultimate wake

Q = propeller torque

r = radial coordinate

r_c = tip vortex core radius

R_R = radius of curvature of helical vortex

R_W = radius of ultimate wake helix

T = propeller thrust

u_a, u_t = axial, tangential induced velocities

$\bar{u}_a, \bar{u}_t$ = normalized axial and tangential induced velocities

V_a = propeller speed of advance

β = geometric advance angle $\tan^{-1} \frac{V_A}{2\pi nr}$

β_i = advance angle including induced velocities from lifting-linfe theory

β_w = advance angle of vortex ultimate wake

Γ = circulation

λ_i = advance coefficient $\frac{r}{R}\tan\beta_i$

η = propeller efficiency $\frac{K_T J}{2\pi K_Q}$

ρ = fluid mass density

ω = propeller rotational speed in radians/second

ACKNOWLEDEMENTS

The author wishes to express his appreciation to S. Dean Lewis, Research Engineer, Michael Fitsgibbons, Research Assistant, and William Connely, Technician for their work in carrying out the experimental portion of this research. The present work is an outgrowth of the Doctoral research carried out at M.I.T. by Theodore Loukakis, currently Professor of Naval Architecture, Faculty of Mechanical and Electrical Engineering, at the National Technical University of Athens, Greece.

I. INTRODUCTION

A major obstacle in obtaining an "exact" numerical solution of the flow around a three-dimensional lifting surface is the difficulty in determining the position of the trailing vortex wake. This problem has the usual difficulties associated with boundary value problems with unknown boundaries, with the additional complication of the essential role of viscosity in the tip vortex core region.

It is fortunate that for many applications a precise knowledge of the geometry of the trailing vortex wake is not essential. The pressure distribution on a three-dimensional planar hydrofoil can be accurately computed, in most cases, with complete neglect of the deformation of the wake. Exceptions to this statement include the determination of the pressure distribution in the immediate vicinity of the tip, or the analysis of low aspect ratio hydrofoils operating with vortex sheet separation from the leading edge.

The problem is more complicated in the case of a propeller. Here the trailing vortices follow a generally helical path downstream, and the velocity which they induce on the blade is significantly altered by a deformation in their trajectory. For example, the velocity induced on one blade by the tip vortex shed from the next blade ahead is roughly proportional to the inverse of the minimum distance between the blade and the vortex. This distance is significantly altered by the combination of axial and radial deformation of the vortex.

This problem had been recognized in the earliest analytical treatments of propeller theory, and the well-known representation of the "moderately loaded propeller" can be thought of

as a deformed wake model [1], [2]. In this case, a very simple deformation is introduced by modifying the pitch of the trailing vortices to match the flow angle computed at a lifting-line with the same radial circulation distribution as the actual propeller. Since the trailing vortices shed at different radii will not necessarily have the same pitch the resulting vortex sheet for downstream will be of continuously changing form.

This model has had the enviable characteristic of getting better with age. When first introduced, computer-aided numerical lifting-surface theory was, of course, not available to determine detailed propeller blade section characteristics for a prescribed loading. Semi-empirical camber and pitch correction factors were, of necessity, employed in determining blade section shape [3], so that errors in the final result could not necessarily be blamed on the wake model. As numerical lifting surface theory progressed in accuracy [4], [5], [6], [7], correlation between theory and experiment became excellent, even though the classic "moderately-loaded" wake model was retained.

It is important to recognize, however, that this model cannot properly represent flow conditions downstream of the propeller. The author must admit falling into this trap in developing a numerical procedure for computing propeller field point velocities [8], [9]. Retention of the "moderately-loaded" wake model, in this case, results in an oscillation in the amplitude of the blade freqeuncy pressure with downstream positions, while both experiment and pure linear theory yield monotonically decreasing amplitudes. On the other hand, correlation between theory and experiment near the propeller, which is generally of primary importance, is extremely satisfactory.

One possible variation on the classical "moderately-loaded" wake model was introduced by Burrill[10]. Recognizing that the velocity induced by a helical vortex is doubled downstream,

the pitch of the helical vortices shed from the blades was appropriately increased. Since the Burrill procedure, which again pre-dated the introduction of digital computers, was handicapped by possible inaccuracies in estimating lifting-surface effects, the final result, as with [3], could not be used to judge the effectiveness of the wake model.

One can conclude, therefore, that the "moderately-loaded" wake model is evidently an effective "substitute vortex system" for the purpose of determining the flow on or near the blade. Viewed in this way, it does not matter whether or not the substitute vortex system deviates significantly from the true vortex wake downstream. Conversely, since it is a substitute, it may lead to wrong answers if used for any other purpose.

Considerable effort has been directed in recent years towards the determination of the true propeller wake geometry. Since a concurrent survey paper by Cummings [11] reviews this work, no attempt will be made here to duplicate this material, except to state the general conclusion. Detailed numerical computations of propeller vortex sheet deformations, while within the realm of possibility for current computers, are probably not worth the effort. At the present time, we are unaware of the existence of any practical working programs for this purpose.

We have therefore pursued a simpler approach which is intermediate between the theory of moderately-loaded propellers and a complete numerical determination of the wake geometry.

II. THE ULTIMATE WAKE MODEL

Observations of propeller tip vortex trajectories in the MIT Variable Pressure Water Tunnel tend to indicate that the roll-up process must be extremely rapid. The slipstream contracts behind the propeller to a constant value which is maintained for the entire length of the test section downstream of the propeller. If any significant amount of vortex roll-up were taking place further downstream, this would be evidenced by a continual change in radius and pitch. It seemed, therefore, that rather than chasing vortices, it would be more efficient to focus attention on the ultimate wake. The ultimate wake would consist of a concentrated helical tip vortex shed from each blade, and a hub vortex coincident with the shaft axis. Since we are looking far downstream, these vortices can be regarded as infinite in extent, so that the problem becomes effectively a two-dimensional one.

The ultimate wake must be joined to the propeller by a "transition wake" region, which is where the complex rolling-up and contracting phenomenon takes place. However, if this region is limited in extent, it can be modelled with sufficient accuracy by a smooth surface consisting of vortex lines shed from the trailing edge and converging at the "roll-up points". This concept is illustrated in Figure 1.

The development of this ultimate wake model was undertaken by Loukakis [12], who developed analytical methods to determine the ultimate wake radius and pitch, and ran a pilot experiment in the water tunnel to measure these quantities. Good agreement was found between theory and experiment. His results showed, in particular, that the ultimate wake radius was practically

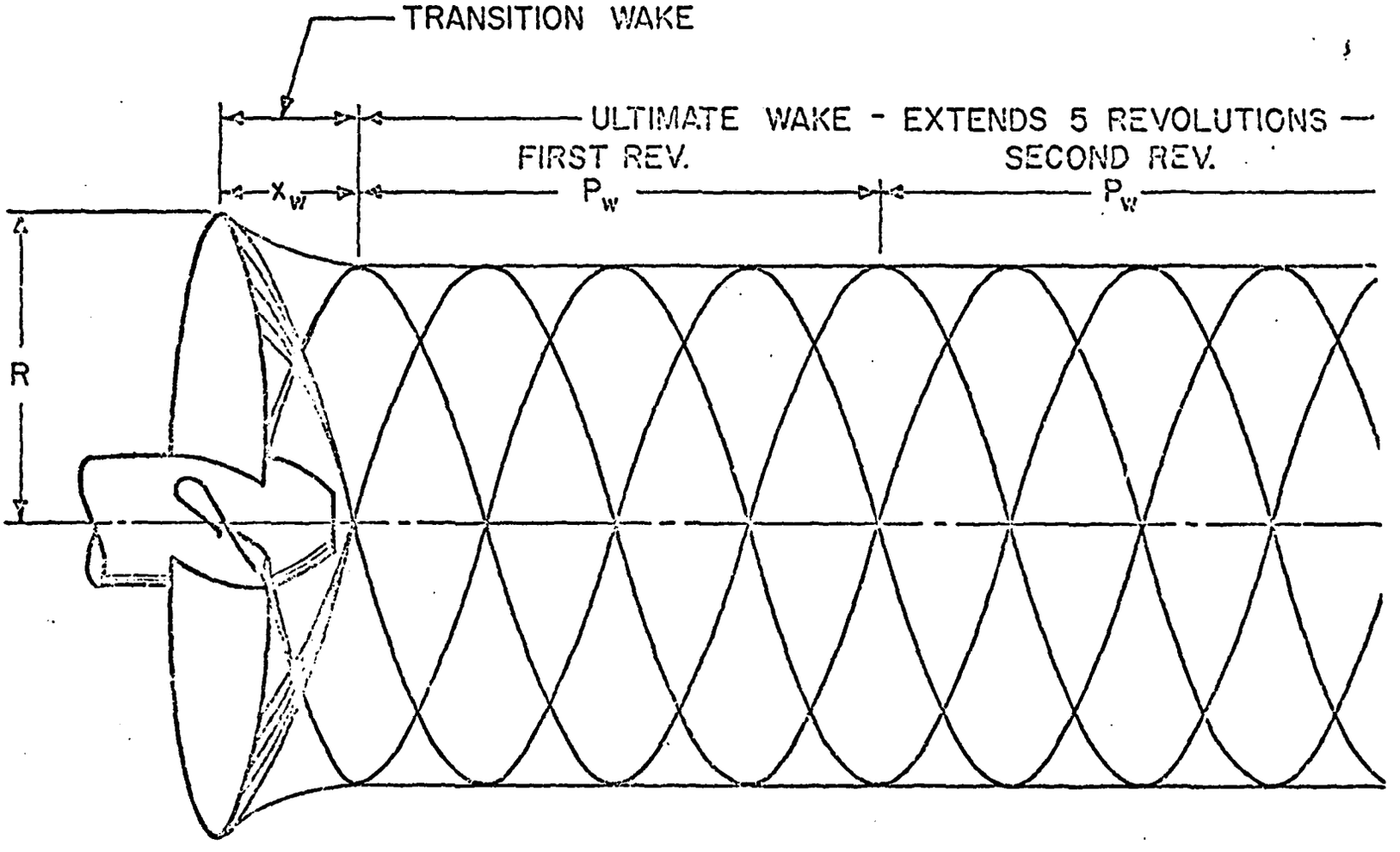

Figure 1. - Schematic of simplified deformed wake model consisting of a transition and an ultimate wake.

independent of propeller loading and that the ultimate wake pitch was less than that predicted by the theory of moderately-loaded propellers. The latter tended to confirm, at least qualitatively, the similar conclusion reached by Cummings [13].

The present research is directed towards the application of this deformed wake model to design, and consists of three parts:

1. A systematic series of measurements of ultimate wake pitch and radius.
2. Correlation of these measurements with theory.
3. Modification of the existing propeller lifting-surface program to include the computation of induced velocities on the blade in accordance with the present deformed wake model.

III. EXPERIMENTAL PROGRAM

A. Performance Tests

A series of four three-bladed propellers were supplied by DTNSRDC for the purpose of this study. The characteristics of the propellers, which all have a pitch/diameter ratio of approximately 1.07, are given in [14]. Figure 2, reproduced from [14], shows the variations in blade outline covered by the series.

In addition, a stock three-bladed motorboat propeller with a pitch/diameter ratio of 0.67 was tested in order to obtain data applicable to propellers with a lower design advance coefficient.

Measurements of thrust coefficient, K_T, torque coefficient, K_Q, and efficiency versus advance coefficient J, were made in the MIT Variable Pressure Water Tunnel under non-cavitating conditions. Following standard procedures, the test RPM was adjusted to provide the highest Reynolds Number possible without exceeding the capacity of the dynamometer or the maximum tunnel flow speed. For these propellers, the range of RPM was from 1000 to 1800, yielding Reynolds Numbers ranging from 2×10^6 to 3.5×10^6.

Faired values of K_T, K_Q, and efficiency corrected for tunnel wall effect at intervals of 0.1 in advance coefficient are given in Tables 1-5. The results for the four series propellers are generally in good agreement with the results of the DTNSRDC open water tests [14].

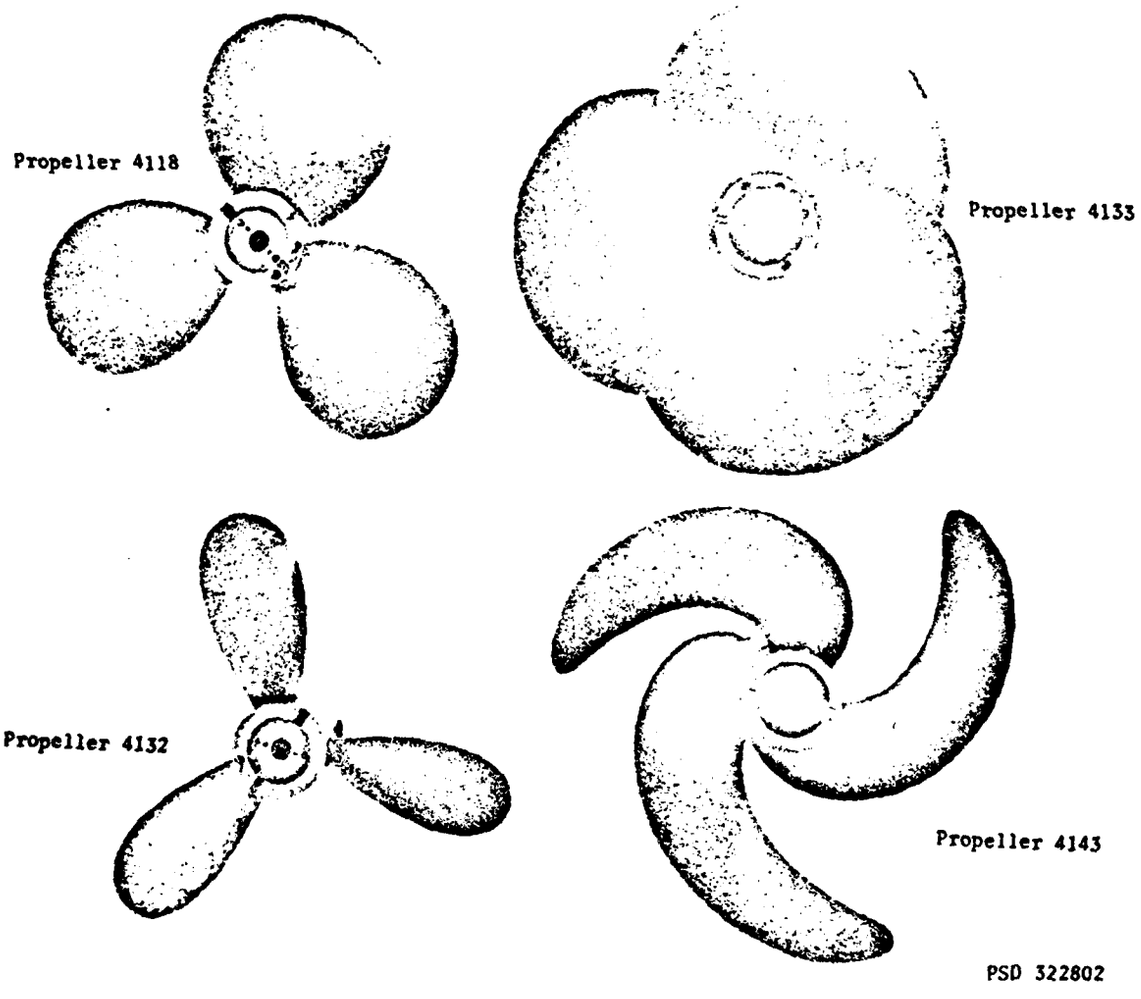

Figure 19 - Propellers 4118, 4132, 4133, 4143

Fig 2. Propellers for hydrofoil noise measurements - (from [143]).

TABLE 1. FAIRED EXPERIMENTAL VALUES OF PROPELLER PERFORMANCE CORRECTED FOR TUNNEL WALL EFFECT FOR DTNSRDC PROPELLER 4118.

J	K_T	K_Q	η
.2	.420	.0675	.198
.3	.381	.0618	.295
.4	.342	.0560	.389
.5	.301	.0501	.478
.6	.257	.0440	.559
.7	.213	.0377	.628
.8	.170	.0318	.682
.9	.129	.0260	.714
1.0	.086	.0195	.700
1.1	.040	.0126	.558
1.2	-.005	.0055	-.224

TABLE 2. FAIRED EXPERIMENTAL VALUES OF PROPELLER PERFORMANCE CORRECTED FOR TUNNEL WALL EFFECT FOR DTNSRDC PROPELLER 4132.

J	K_T	K_Q	η
.2	.337	.0472	.227
.3	.310	.0444	.333
.4	.283	.0416	.434
.5	.255	.0386	.526
.6	.226	.0355	.608
.7	.195	.0321	.676
.8	.163	.0285	.729
.9	.133	.0246	.773
1.0	.100	.0199	.804
1.1	.064	.0142	.793
1.2	.026	.0080	.628
1.3	-.013	.0014	-1.904

TABLE 3. FAIRED EXPERIMENTAL VALUES OF PROPELLER PERFORMANCE CORRECTED FOR TUNNEL WALL EFFECT FOR DTNSRDC PROPELLER 4133

J	K_T	K_Q	η
.2	.523	.0894	.186
.3	.467	.0805	.277
.4	.411	.0717	.365
.5	.354	.0628	.449
.6	.296	.0536	.526
.7	.237	.0445	.593
.8	.182	.0361	.643
.9	.130	.0282	.660
1.0	.079	.0208	.605
1.1	.028	.0135	.357
1.2	-.024	.0062	-.738

TABLE 4. FAIRED EXPERIMENTAL VALUES OF PROPELLER PERFORMANCE CORRECTED FOR TUNNEL WALL EFFECT FOR DTNSRDC PROPELLER 4143.

J	K_T	K_Q	η
.2	.419	.0629	.212
.3	.373	.0568	.314
.4	.328	.0506	.412
.5	.282	.0445	.505
.6	.236	.0383	.588
.7	.190	.0323	.656
.8	.148	.0267	.704
.9	.110	.0217	.724
1.0	.071	.0167	.682
1.1	.032	.0116	.487
1.2	-.007	.0065	.214

TABLE 5. FAIRED EXPERIMENTAL VALUES OF PROPELLER PERFORMANCE CORRECTED FOR TUNNEL WALL EFFECT FOR 12 × 8 STOCK PROPELLER.

J	K_T	K_Q	η
.1	.266	.0294	.144
.2	.229	.0264	.281
.3	.192	.0226	.406
.4	.152	.0190	.510
.5	.113	.0154	.582
.6	.074	.0116	.605
.7	.030	.0072	.462
.8	-.016	.0025	-.839

B. Measurement of Tip Vortex Trajectories

The MIT Variable Pressure Water Tunnel is particularly well suited for the measurement of propeller tip vortices, due to its square test section, with one long unobstructed plexiglass window on each side. The propeller can be located in the forward portion of the test section, thus leaving sufficient distance downstream for observation of the tip vortices. The tunnel pressure can be adjusted to provide the minimum amount of tip vortex cavitation to permit observation.

The initial experiment conducted by Loukakis [12] was done, of necessity, in the simplest possible way. A sighting device was made by gluing together three plastic drafting triangles. This device was held firmly against the test section window, and the tip vortices were traced by sighting along the edge of the device normal to the window.

For the present study, an improved sighting instrument was devised. This consisted of a ten-power telescopic sight attached to a drafting machine which, in turn, was securely attached to the tunnel test section. The telescopic sight could be moved along a tip vortex with great precision, and the horizontal and vertical coordinates of a set of points could be read directly on the drafting machine scales. A photograph of this equipment in operation appears in Figure 2. With the telescope centered on a vortex, it was immediately apparent that tunnel pressure could be changed considerably before any alteration in the position of the vortex occurred.

The data was analysed by fitting the best least-squares helix through the measured points. This is equivalent to the problem of obtaining the amplitude and phase of a harmonic function of unknown wave length. The procedure is to assume the wavelength, i.e. the pitch of the helix, solve for the amplitude and phase of the fundamental by the usual technique

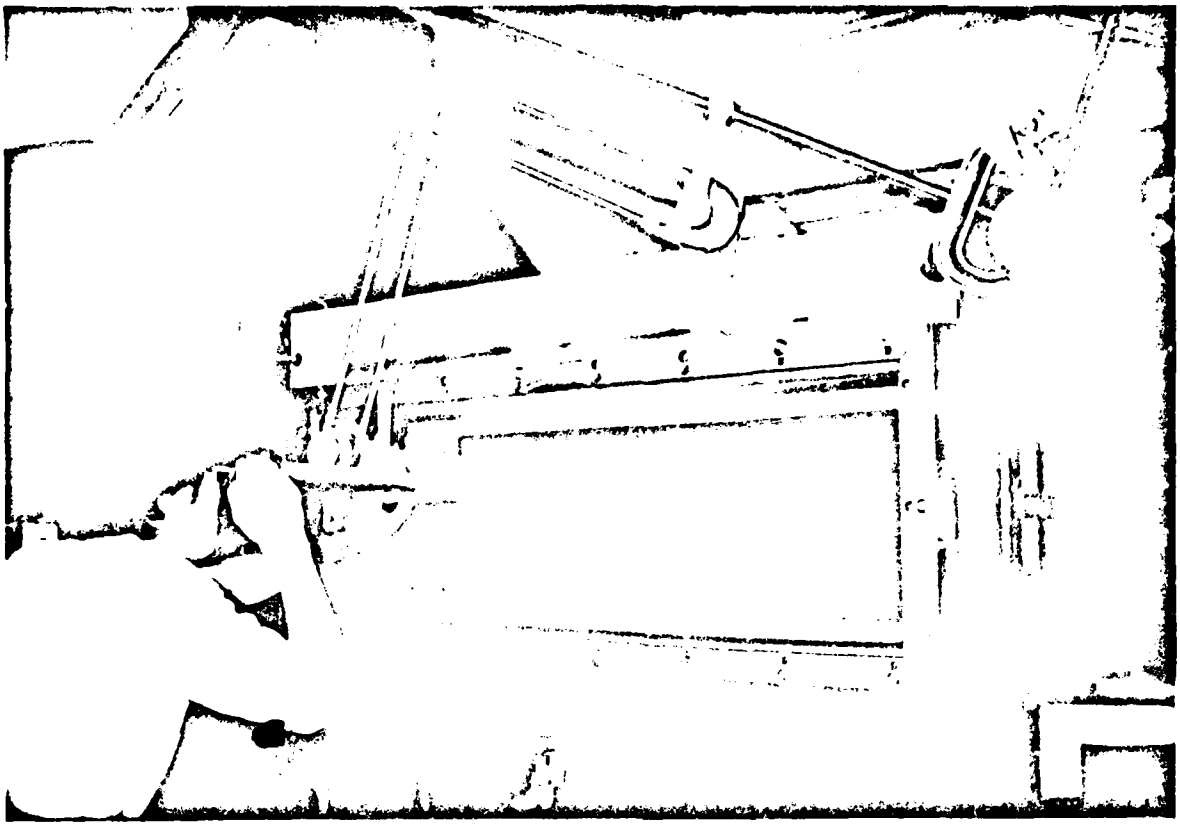

Figure 2. - Photograph of telescopic sighting device for the measurement of tip vortex trajectories.

of discrete harmonic analysis, and compute the mean-squared error. The wave-length is then altered slightly, and the harmonic analysis and error calculation is repeated. An iterative procedure is then followed to determine the wavelength for minimum error.

A typical computer output is shown in Figure 3. This consists of a tabulation of input coordinates, a plot of the original data together with the least-squares helix, and a tabulation of the final pitch, radius and phase of the helix. In almost all cases, the helix provided an extremely close approximation to the measured data.

It was found that the accuracy of these measurements was very dependent upon the quality of the propeller models. If the blades were not all identical, the wake would become progressively more distorted downstream. The hub vortex, in this case, would not remain on the axis, but would be attracted towards one tip vortex, and in the process would develop a helical shape with increasing radius. Eventually, this would cause complete breakdown of the original tip vortices.

While some laboratory model propellers tested were far more symmetrical, the differences in pitch of the tip vortices from each blade could readily be measured. Some models were clearly superior to others in this respect. This effect was particularly noticeable for the stock motorboat propeller, where one would not expect laboratory standard tolerances.

To obtain the best average value of the ultimate wake pitch and radius, measurements were made of the tip vortex from each blade set at both zero and ninety degrees by means of the phase of the strobe-light.

The results are given in Figures 4-7 for a series of four three-bladed propellers designed by DTNSRDC [14]. The curve labeled "initial pitch" is the axial distance from the tip of the blade to the first revolution of the tip vortex. The

```
 DEFORMED WAKES INPUT DATA
PROP. 4133   TEST  24   BLADE  3    90                    24 JULY 72

ROOM TEMPERATURE =   P4  TUNNEL TEMPERATURE =   90  MANOMETER =    867.00  TAP CODE =  1/  1
PROPELLER DIAMETER =  12.00  RPM = 1165.00  TORQUE =  500.50  THRUST =  232.50
XI=  669.00  YI=  431.00  XR=  647.00  YR=  137.00
XL=  820.00  YM=  284.00  XM=  648.00

    650.00    336.00
    660.00    305.00
    670.00    271.00
    680.00    238.00
    690.00    209.00
    700.00    190.00
    710.00    181.00
    720.00    179.00
    728.00    185.00
    740.00    191.00
    750.00    186.00
    760.00    195.00
    770.00    211.00
    780.00    242.00
    795.00    296.00
    810.00    335.00
    820.00    362.00
    830.00    386.00
    840.00    403.00
    850.00    414.00
    860.00    420.00
    870.00    419.00
    880.00    405.00
    893.00    386.00
    900.00    363.00
    910.00    336.00
    920.00    303.00
    930.00    272.00
    940.00    240.00
    950.00    211.00
    960.00    187.00
    970.00    169.00
    980.00    158.00
    991.00    154.00
   1000.00    159.00
   1010.00    170.00
   1020.00    188.00
   1030.00    210.00
   1040.00    237.00
   1050.00    268.00
   1060.00    298.00
   1070.00    328.00
   1080.00    355.00
   1090.00    381.00
   1100.00    399.00
   1110.00    413.00
   1120.00    420.00
   1130.00    416.00
   1140.00    407.00
```

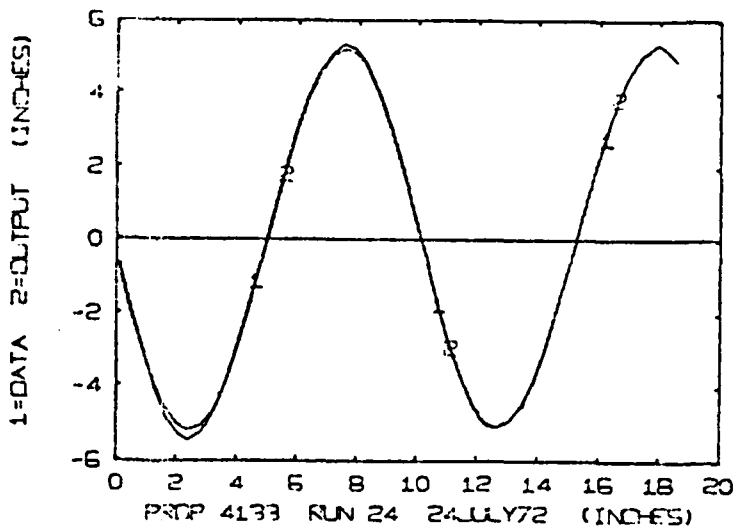


```
THE WAVELENGTH IS   260.319

THE AMPLITUDE IS    132.31  THE PHASE SHIFT IS      3.21
WATER VELOCITY =  12.07  THE UNCORRECTED J IS  0.621

THE WAKE HAS A PITCH VALUE OF  10.24 IN., A RADIUS VALUE OF   5.20 IN.

          WITH AN OFFSET OF   7.57 IN.
```

Figure 3. - Sample computer output of vortex curve-fitting procedure.

ultimate pitch P_W, is the pitch of the tip vortex measured as far downstream in the test section as possible. At the design advance coefficient, $J = 0.833$, the average initial pitch was three percent less than the ultimate pitch. This extremely small difference is one indication that vortex sheet roll-up is extremely rapid, and that one does not have to proceed very far downstream to reach the ultimate wake.

The two dotted lines plotted in Figures 4-7 are, respectively, the pitch of the undisturbed flow

$$P_o = 2\pi r \tan \beta \ , \qquad (1)$$

and the pitch of the tip vortex in accordance with the theory of moderately loaded propellers

$$P_i = 2\pi r \tan \beta_i \ . \qquad (2)$$

The latter was obtained from a lifting-line theory calculation with the measured thrust as input, assuming that the radial distribution of circulation was optimum.

In all cases, the ultimate wake pitch falls almost exactly midway between these two limits.

The ultimate wake radius is plotted at the bottom of Figures 4-7 and can be seen to be essentially independent of propeller loading, with a mean value of 83% of the propeller radius. Subsequent observations of a number of propellers with varying geometry and number of blades have been made, and the ultimate wake radius is generally very close to 83%. However, at extremely high trust coefficients, one can observe a dependence of ultimate wake radius on loading, with values falling below 83%. Some indication of this trend is apparent from Figures 4-7.

Figure 4

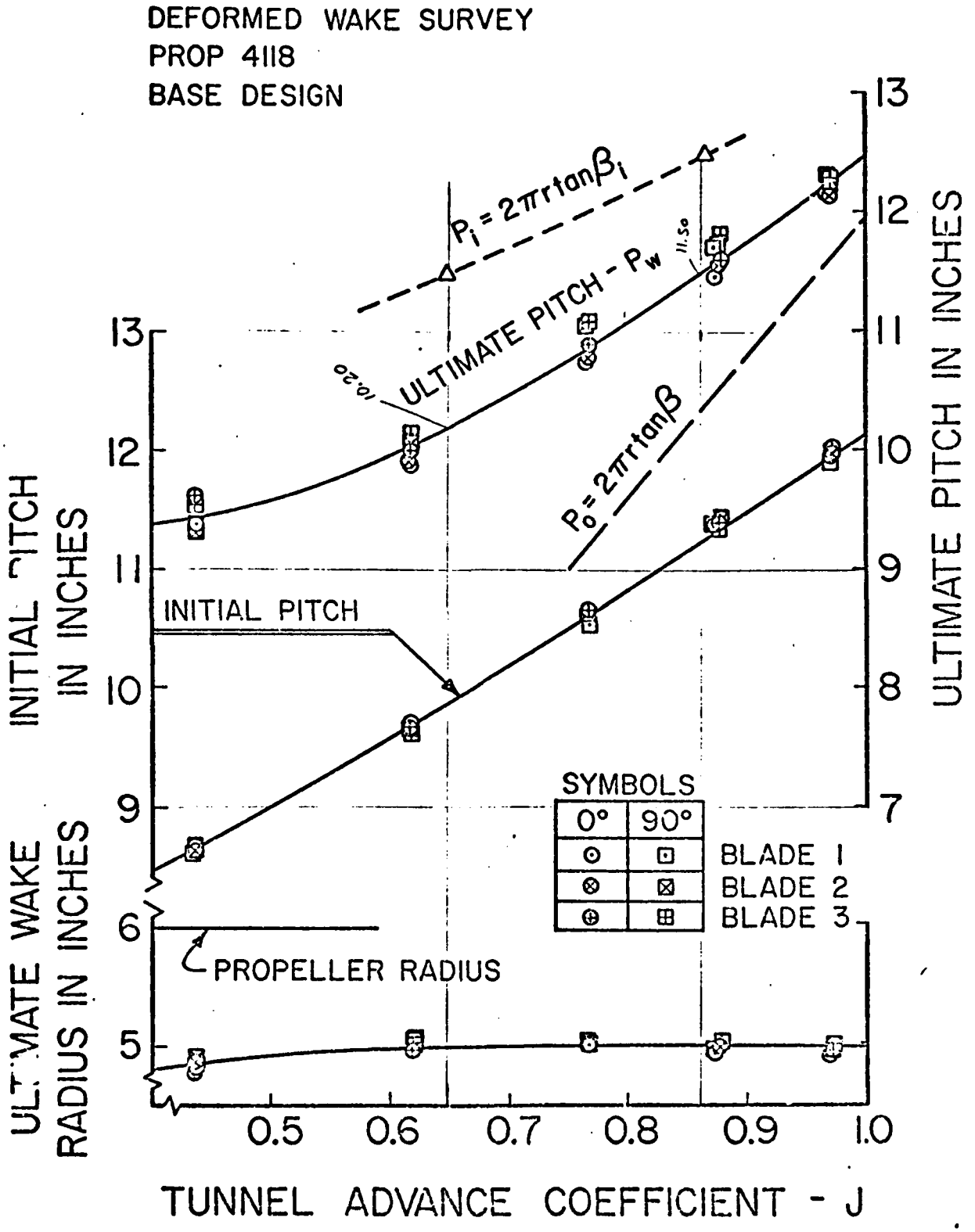
DEFORMED WAKE SURVEY
PROP 4118
BASE DESIGN
$P_i = 2\pi r \tan\beta_i$
ULTIMATE PITCH - P_w
$P_o = 2\pi r \tan\beta$
INITIAL PITCH
PROPELLER RADIUS
SYMBOLS
0°
90°
BLADE 1
BLADE 2
BLADE 3
ULTIMATE WAKE RADIUS IN INCHES
INITIAL PITCH IN INCHES
ULTIMATE PITCH IN INCHES
TUNNEL ADVANCE COEFFICIENT - J
0.5
0.6
0.7
0.8
0.9
1.0
5
6
7
8
9
10
11
12
13

Figure 5

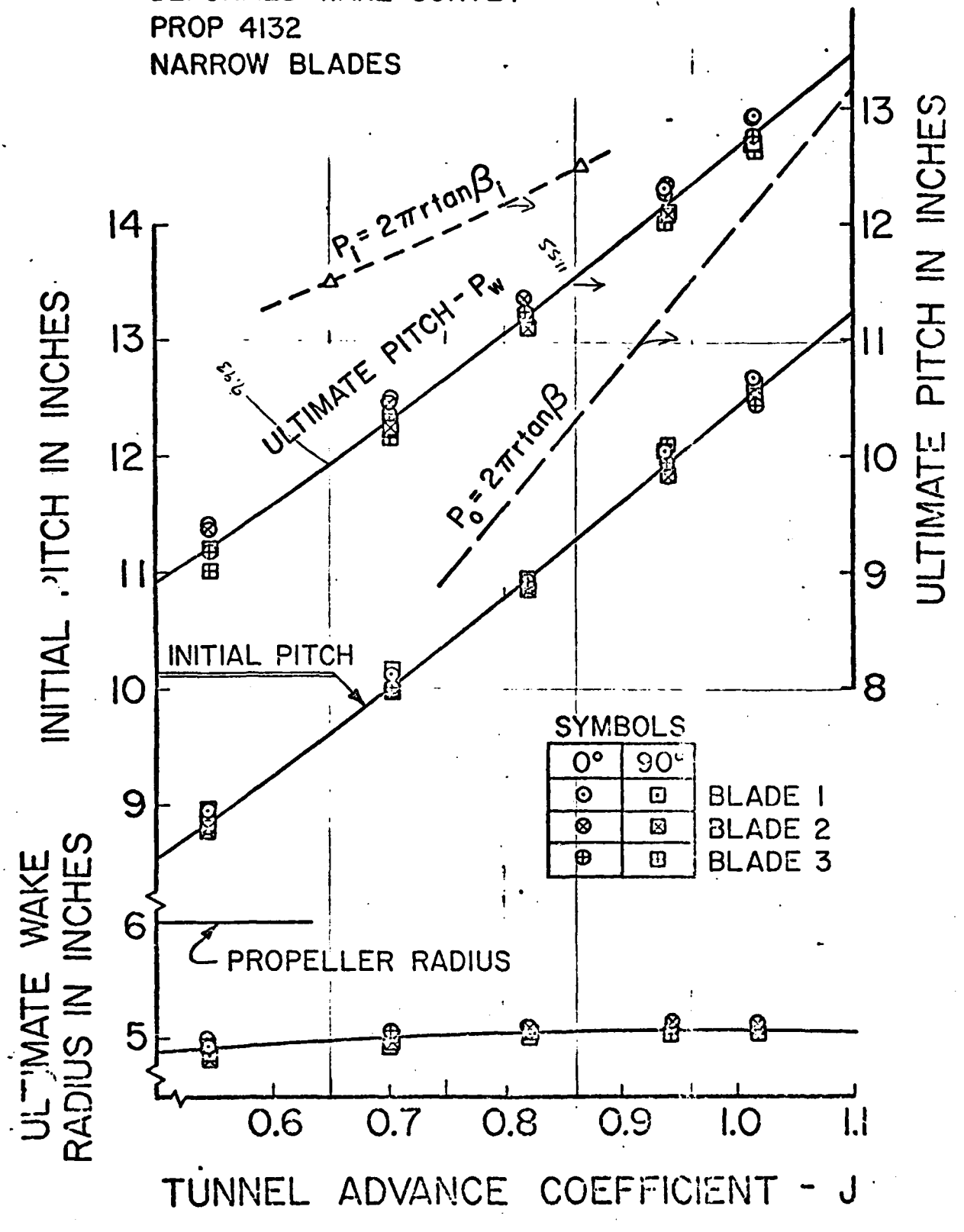
DEFORMED WAKE SURVEY
PROP 4132
NARROW BLADES
INITIAL PITCH IN INCHES
ULTIMATE PITCH IN INCHES
ULTIMATE WAKE RADIUS IN INCHES
TUNNEL ADVANCE COEFFICIENT - J
$P_I = 2\pi r \tan\beta_I$
$P_o = 2\pi r \tan\beta$
ULTIMATE PITCH - P_w
INITIAL PITCH
PROPELLER RADIUS
0.7R
1.15
SYMBOLS
0°
90°
BLADE 1
BLADE 2
BLADE 3
14
13
12
11
10
9
6
5
0.6
0.7
0.8
0.9
1.0
1.1
13
12
11
10
9
8

Figure 6

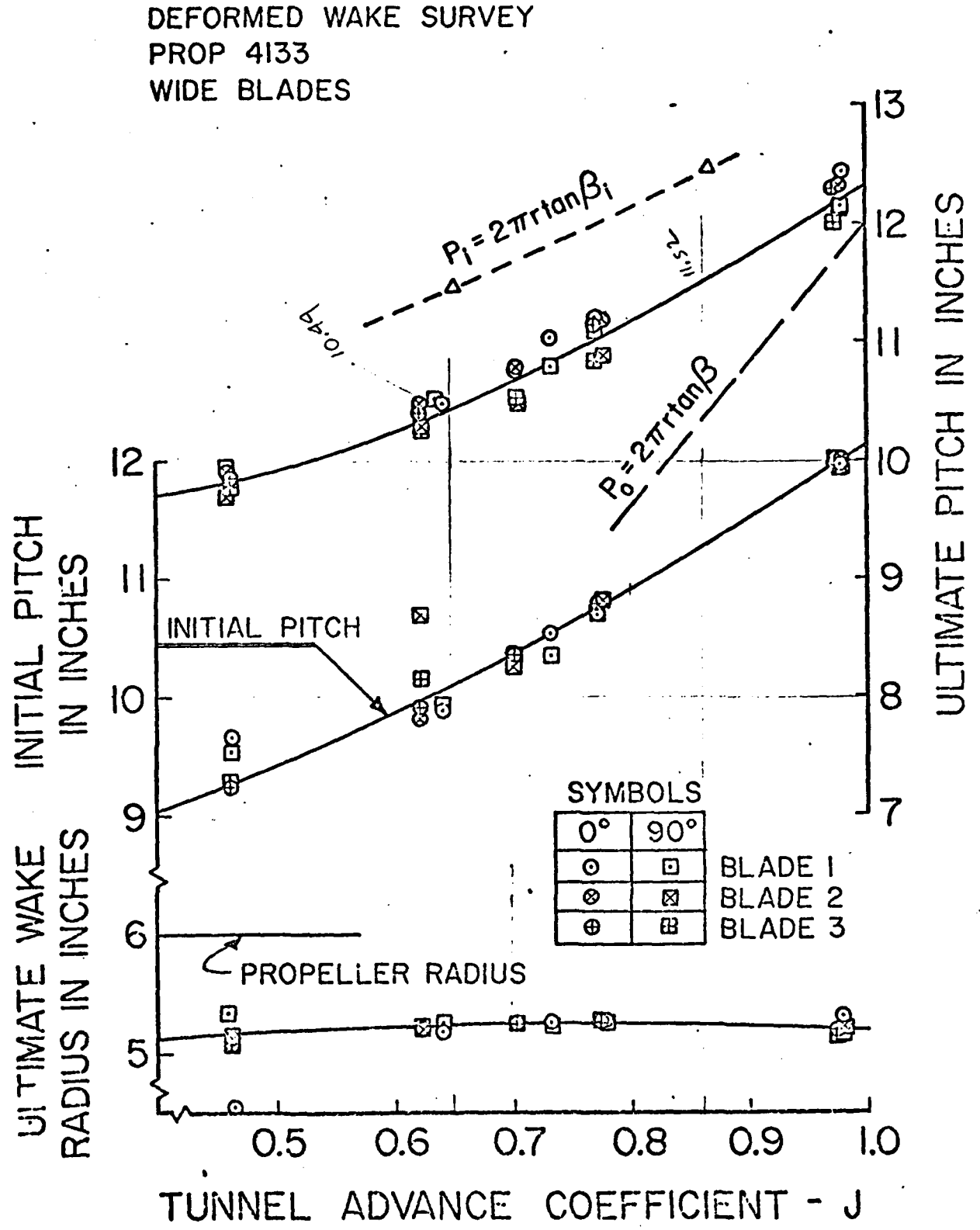
DEFORMED WAKE SURVEY
PROP 4133
WIDE BLADES
$P_i = 2\pi r \tan\beta_i$
$P_o = 2\pi r \tan\beta$
10.49
11.27
INITIAL PITCH
PROPELLER RADIUS
SYMBOLS
0°
90°
BLADE 1
BLADE 2
BLADE 3
ULTIMATE WAKE INITIAL PITCH RADIUS IN INCHES
ULTIMATE PITCH IN INCHES
TUNNEL ADVANCE COEFFICIENT - J
0.5
0.6
0.7
0.8
0.9
1.0
5
6
7
8
9
10
11
12
13

Figure 7

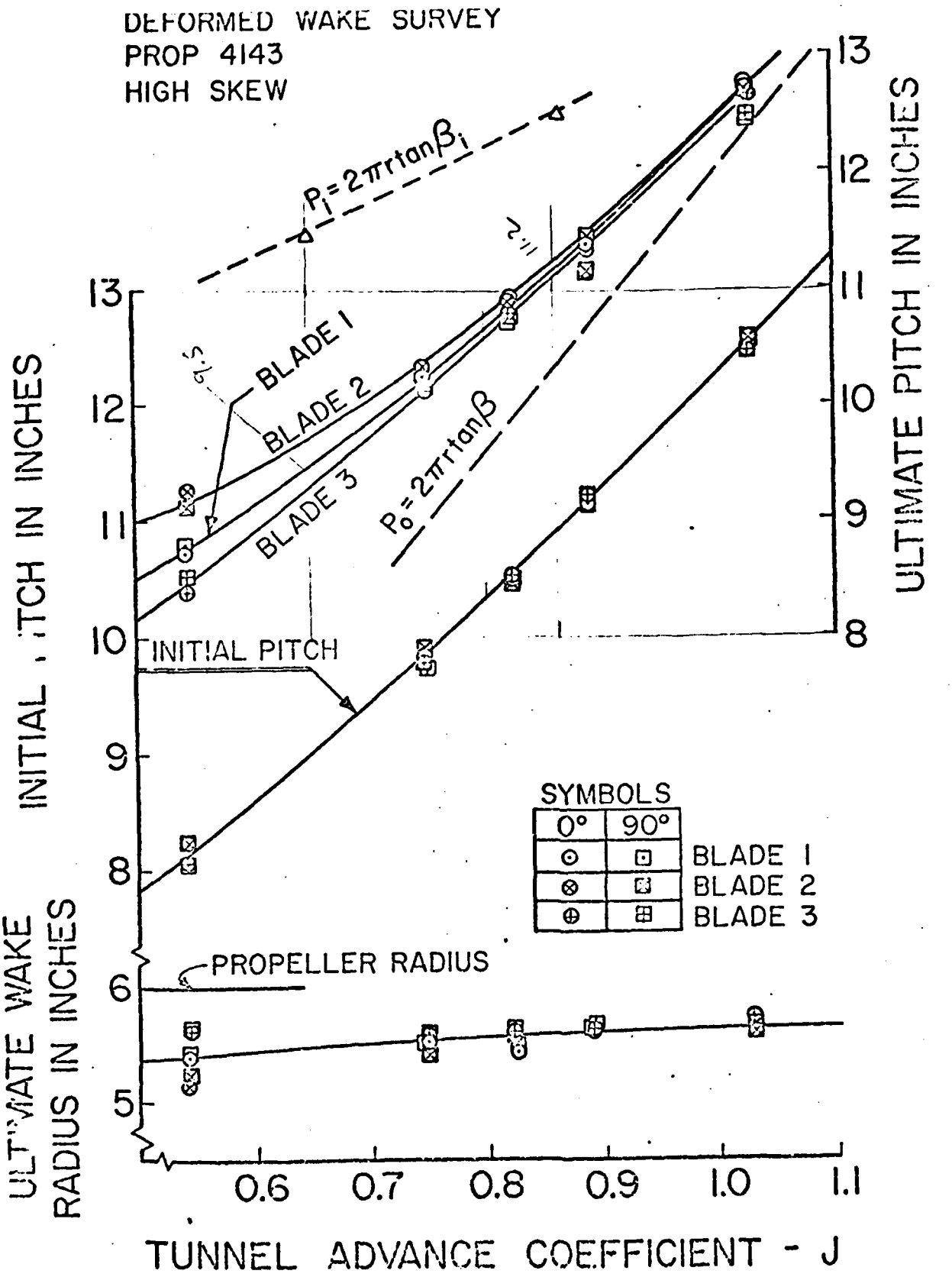
DEFORMED WAKE SURVEY
PROP 4143
HIGH SKEW
$P_i = 2\pi r \tan\beta_i$
$P_o = 2\pi r \tan\beta$
BLADE 1
BLADE 2
BLADE 3
INITIAL PITCH
PROPELLER RADIUS
SYMBOLS
0°
90°
BLADE 1
BLADE 2
BLADE 3
INITIAL PITCH IN INCHES
ULTIMATE PITCH IN INCHES
ULTIMATE WAKE RADIUS IN INCHES
TUNNEL ADVANCE COEFFICIENT - J
0.6
0.7
0.8
0.9
1.0
1.1
5
6
8
9
10
11
12
13

IV. COMPUTATION OF THE ULTIMATE WAKE PITCH

A. Discrete Helical Vortices

It is assumed that all vorticity rolls up into discrete tip vortices and a hub vortex, in a relatively short distance behind the propeller. In the ultimate wake, we then have a flow consisting of set of infinite helical vortex cores, and an infinite straight hub vortex core. The core radius, r_c, is assumed to be known.

The self-induced velocity of a set of K infinite helical vortex can be expressed as follows,

$$u_a = \bar{u}_a(\beta_w, r_c, K)\ \frac{\Gamma}{R_w}$$

$$u_t = \bar{u}_t(\beta_w, r_c, K)\ \frac{\Gamma}{R_w}\ , \qquad (3)$$

where R_w is the radius of the helix, with pitch

$$P_w = 2\pi R_w \tan\beta_w\ . \qquad (4)$$

Γ is the circulation, and r_c is the core radius non-dimensionalized on the radius of the helix. The functions $\bar{u}_a$ and $\bar{u}_t$ contain a logarithmic singularity as $r_c \to 0$, so that the assumption of a finite core size is essential.

Numerical values for $\bar{u}_a$ and $\bar{u}_t$ may be computed in two parts. The part of the helix close to the point where we are computing the velocity is approximated by a segment of a circular vortex with radius equal to the radius of curvature of the helix. As shown, for example, by Lamb [15], this yields a velocity normal to the helix of magnitude

$$\delta\bar{u}_r = \frac{\Gamma}{4\pi R_R} \log\left(1.576 \frac{R_R\phi}{r_c R_w}\right) , \qquad (5)$$

where 2ϕ is the included angle of the segment, and R_R is the radius of the tangent ring,

$$R_R = R_w/\cos^2\beta_w . \qquad (6)$$

The velocity induced by the rest of the first helix, and from the entire remaining K-1 helices, may be obtained by numerical integration of the usual Biot-Savart Law integral for zero core size. Numerical experimentation indicates that the answer is insensitive to the choice of 2ϕ when the length of the ring segment is varied from 4-20 times the core radius.

Calculations of $\bar{u}_a$ and $\bar{u}_t$ for various values of β_w, r_c and K are given by Loukakis [12] in Tables 6-7 and Figures 8-9, which are reproduced here.

The hub vortex induces a tangential velocity, independent of core size

$$\bar{u}_t = \frac{-K\Gamma}{2\pi R_w} . \qquad (7)$$

The requirement that the tip vortex helix be a streamline leads to the following equation for β_w:

$$\tan\beta_w = \frac{V_A + \bar{u}_a(\beta_w, r_c, K) \cdot \Gamma/R_w}{\omega R_w - \frac{-K\Gamma}{2\pi R_w} + \bar{u}_t(\beta_w, r_c, K) \cdot \Gamma/R_w} . \qquad (8)$$

The ultimate wake pitch may therefore be computed by an iterative procedure from (8) once the wake radius and core size is given. Loukakis [12] has shown that if the propeller thrust is known, a momentum balance can be used to obtain one more relationship between pitch and radius, thus permitting a solution for both quantities. However, we can avoid this

AXIAL AND TANGENTIAL SELF-INDUCED VELOCITIES - INFINITE HELICES										
tanβ	K = 1		K = 2		K = 3		K = 4		K = 5	
	UA	UT	UA	UT	UA	UT	UA	UT	UA	UT
0.10	0.9800	0.0353	1.7169	0.1261	2.4920	0.2664	3.2513	0.2893	4.0256	0.4223
0.15	0.7416	0.0200	1.2162	0.1116	1.7158	0.2114	2.2191	0.2784	2.7277	0.3700
0.20	0.6234	0.0009	0.9668	0.0931	1.3326	0.1830	1.7059	0.2622	2.0835	0.3459
0.25	0.5503	-0.0185	0.8161	0.0748	1.1029	0.1628	1.3978	0.2457	1.6969	0.3286
0.30	0.4980	-0.0370	0.7131	0.0576	0.9479	0.1457	1.1907	0.2302	1.4377	0.3134
0.35	0.4564	-0.0539	0.6364	0.0419	0.8347	0.1305	1.0405	0.2158	1.2504	0.2996
0.40	0.4210	-0.0690	0.5757	0.0277	0.7470	0.1169	0.9254	0.2028	1.1076	0.2870
0.45	0.3896	-0.0820	0.5252	0.0153	0.6760	0.1049	0.8333	0.1912	0.9943	0.2757
0.50	0.3611	-0.0930	0.4820	0.0047	0.6166	0.0947	0.7574	0.1812	0.9015	0.2659
0.60	0.3103	-0.1092	0.4103	-0.0114	0.5215	0.0789	0.6379	0.1657	0.7571	0.2505
0.70	0.2665	-0.1189	0.3523	-0.0214	0.4474	0.0688	0.5468	0.1555	0.6487	0.2403
0.80	0.2287	-0.1234	0.3043	-0.0266	0.3877	0.0633	0.4747	0.1498	0.5637	0.2343
0.90	0.1962	-0.1141	0.2641	-0.0280	0.3386	0.0613	0.4161	0.1474	0.4954	0.2316
1.00	0.1686	-0.1221	0.2304	-0.0269	0.2978	0.0619	0.3678	0.1475	0.4394	0.2313
1.25	0.1165	-0.1109	0.1674	-0.0177	0.2223	0.0696	0.2790	0.1540	0.3367	0.2368
1.50	0.0823	-0.0967	0.1258	-0.0054	0.1723	0.0805	0.2201	0.1637	0.2687	0.2456
1.75	0.0595	-0.0832	0.0976	0.0065	0.1381	0.0912	0.1795	0.1735	0.2215	0.2546
2.0	0.0441	-0.0715	0.0780	0.0170	0.1139	0.1007	0.1505	0.1822	0.1875	0.2636
3.0	0.0163	-0.0408	0.0401	0.0441	0.0647	0.1252	0.0897	0.2048	0.1148	0.2836
4.0	0.0076	-0.0258	0.0259	0.0571	0.0447	0.1370	0.0637	0.2156	0.0826	0.2937
5.0	0.0042	-0.0177	0.0190	0.0640	0.0342	0.1431	0.0494	0.2213	0.0647	0.2990
6.0	0.0025	-0.0129	0.0150	0.0680	0.0277	0.1467	0.0405	0.2246	0.0532	0.3020
7.0	0.0016	-0.0098	0.0124	0.0705	0.0234	0.1489	0.0343	0.2266	0.0453	0.3039
8.0	0.0011	-0.0077	0.0106	0.0722	0.0202	0.1504	0.0298	0.2279	0.0394	0.3052
9.0	0.0008	-0.0063	0.0093	0.0734	0.0178	0.1515	0.0264	0.2289	0.0349	0.3060
10.0	0.0006	-0.0052	0.0083	0.0742	0.0160	0.1522	0.0236	0.2296	0.0313	0.3067

Table 6. - Self-induced velocities as a function of number of blades. Ratio of core radius to vortex radius is 1/50. [From Loukakis (12)]

AXIAL AND TANGENTIAL SELF-INDUCED VELOCITIES - INFINITE HELIX								
tanβ	$Rw/r_c = 10$		Rw/r_c		Rw/r_c		Rw/r_c	
	UA	UT	UA	UT	UA	UT	UA	UT
0.10	0.8540	0.0494	0.9257	0.0411	0.9800	0.0353	1.0343	0.0297
0.15	0.6177	0.0397	0.6882	0.0283	0.7416	0.0200	0.7949	0.0118
0.20	0.5026	0.0257	0.5714	0.0115	0.6234	0.0009	0.6754	-0.0096
0.25	0.4333	0.0112	0.4999	-0.0058	0.5503	-0.0185	0.6007	-0.0312
0.30	0.3854	-0.0029	0.4495	-0.0224	0.4980	-0.0370	0.5465	-0.0516
0.35	0.3487	-0.0160	0.4100	-0.0376	0.4564	-0.0539	0.5028	-0.0702
0.40	0.3185	-0.0278	0.3769	-0.0513	0.4210	-0.0690	0.4652	-0.0867
0.45	0.2925	-0.0382	0.3478	-0.0631	0.3896	-0.0820	0.4315	-0.1008
0.50	0.2694	-0.0471	0.3216	-0.0732	0.3611	-0.0930	0.4006	-0.1127
0.60	0.2296	-0.0607	0.2756	-0.0883	0.3103	-0.1092	0.3451	-0.1301
0.70	0.1961	-0.0696	0.2362	-0.0976	0.2665	-0.1189	0.2969	-0.1401
0.80	0.1677	-0.0746	0.2024	-0.1024	0.2287	-0.1234	0.2549	-0.1444
0.90	0.1437	-0.0767	0.1736	-0.1037	0.1962	-0.1241	0.2189	-0.1444
1.00	0.1233	-0.0768	0.1491	-0.1026	0.1686	-0.1221	0.1881	-0.1416
1.25	0.0853	-0.0718	0.1031	-0.0941	0.1165	-0.1109	0.1300	-0.1277
1.50	0.0604	-0.0640	0.0729	-0.0826	0.0823	-0.0967	0.0917	-0.1109
1.75	0.0439	-0.0559	0.0528	-0.0714	0.0595	-0.0832	0.0663	-0.0950
2.0	0.0327	-0.0485	0.0392	-0.0616	0.0441	-0.0715	0.0490	-0.0813
3.0	0.0123	-0.0286	0.0146	-0.0356	0.0163	-0.0408	0.0181	-0.0460
4.0	0.0058	-0.0185	0.0068	-0.0226	0.0076	-0.0258	0.0084	-0.0290
5.0	0.0032	-0.0129	0.0037	-0.0156	0.0042	-0.0177	0.0046	-0.0198
6.0	0.0019	-0.0095	0.0023	-0.0114	0.0025	-0.0129	0.0028	-0.0144
7.0	0.0013	-0.0073	0.0015	-0.0087	0.0016	-0.0098	0.0018	-0.0109
8.0	0.0009	-0.0058	0.0010	-0.0069	0.0011	-0.0077	0.0012	-0.0086
9.0	0.0006	-0.0047	0.0007	-0.0056	0.0008	-0.0063	0.0009	-0.0069
10.0	0.0005	-0.0039	0.0005	-0.0046	0.0006	-0.0052	0.0006	-0.0057

Table 7. - Self-induced velocities as a function of core radius. [From Loukakis (12)]

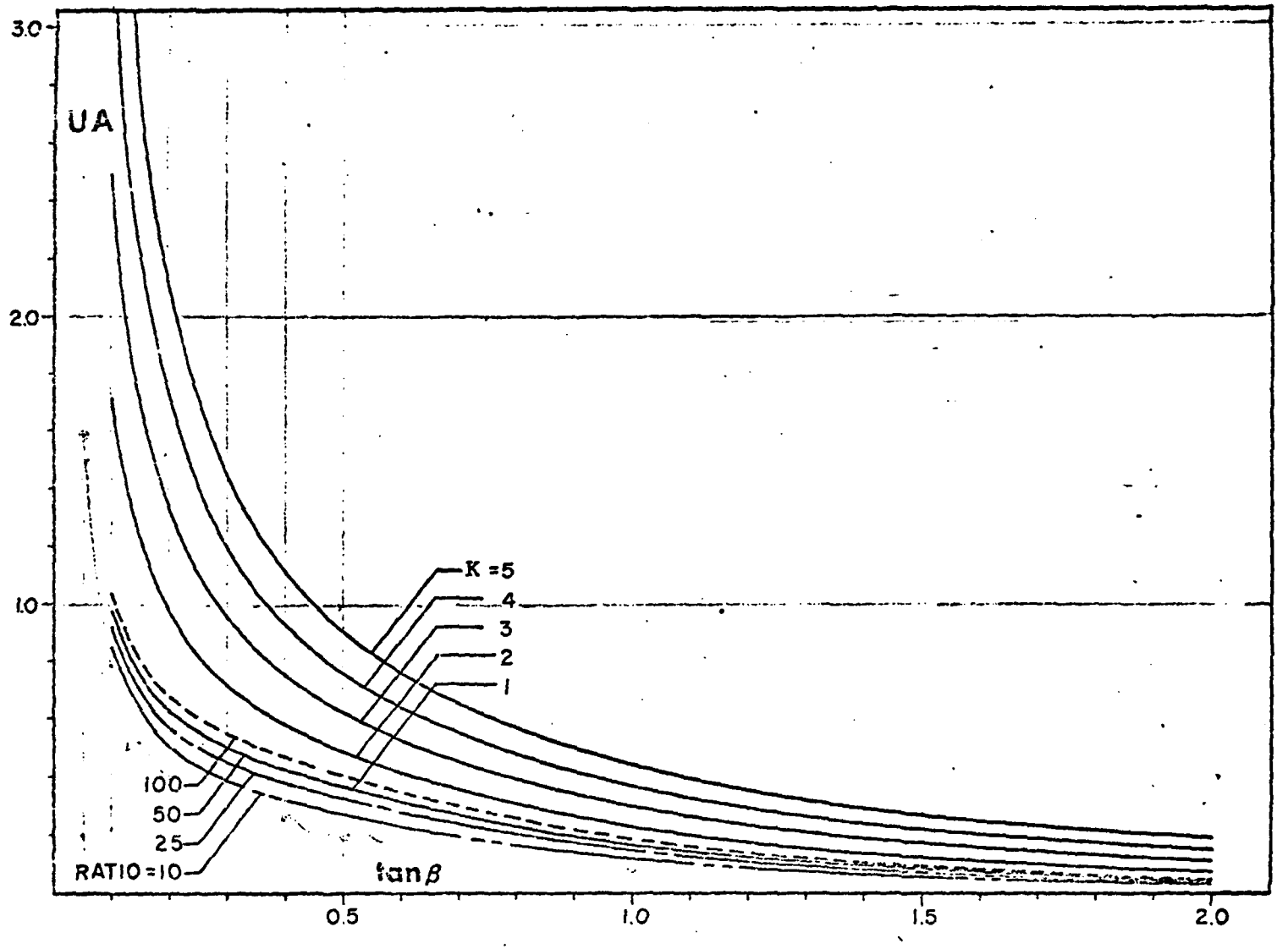

Figure 8. - Axial self-induced velocities. [From Loukakis(12)]

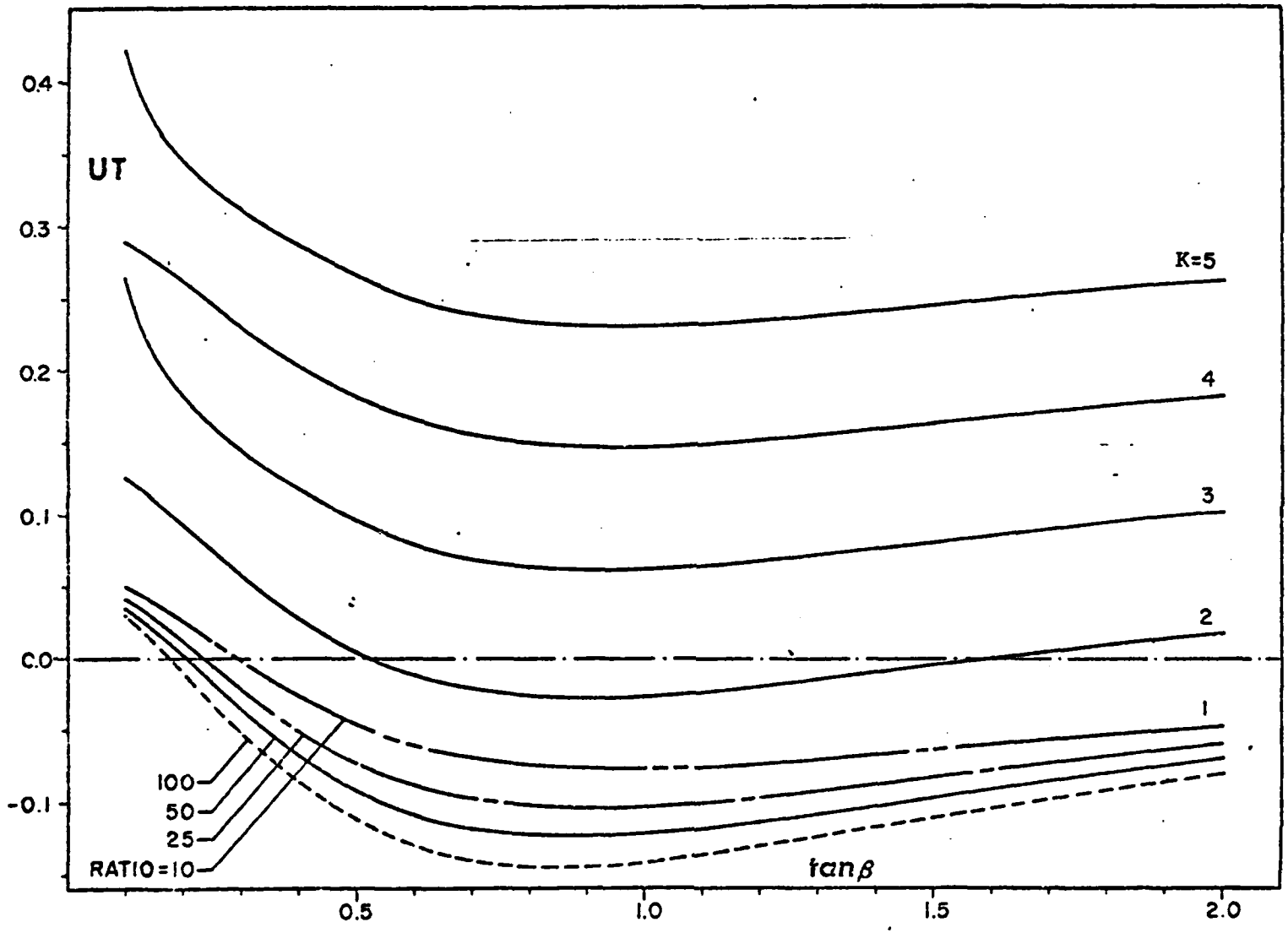

Figure 9. - Tangential self-induced velocities. [From Loukakis (12)]

complication if we are willing to assume a value for ultimate wake radius at the outset. On the basis of our experiments, it would seem that this could be assumed to be 83% of the propeller radius for all applications to light or moderately loaded propellers.

In either case, we must still assume a core radius. The sensitivity of this variable can be judged from Loukakis' calculations plotted in Figures 8-9 for assumed values of core radius ranging from one to ten percent of the vortex radius. Since the contribution of only one blade is affected, precise knowledge of the actual core radius is not critical, particularly for propellers with large numbers of blades.

To compare results obtained in this way with the experiments, it is necessary to make allowance for the influence of the tunnel walls on the pitch and radius of the ultimate wake.

An estimate of the change in pitch can be made by considering the backflow velocity induced by the tunnel walls, This backflow evaluated in the plane of the propeller is the basis for correcting the advance coefficient in the tunnel to match that of an open-water test. This correction was derived for an actuator disc by Glauert [16]. B. D. Cox [17] computed the backflow for a lifting-surface representation of the propeller using the MIT field point program, and found that for the large clearances present in a usual tunnel test that the results were essentially the same. The classical Glauert correction has therefore been built-in to the propeller data reduction program used at MIT.

The corrected tunnel advance coefficient equalizes the inflow in the plane of the propeller in the tunnel and in open water. However, since the backflow velocity doubles downstream, the pitch of the ultimate wake will be reduced by the ratio of this change in backflow to the velocity in the plane of the propeller. This correction, which is a function of propeller-loading, may be obtained from the processed performance data.

An estimate of the influence of the tunnel walls on the radius of the ultimate wake can also be made by comparing the results of an actuator disc in an unlimited fluid with an actuator disc in an infinite cylinder. The following results are obtained for a 12-inch diamter propeller in a 20×20 inch test section with a thrust coefficient $C_T = 0.565$.

Actuator Disc in Unlimited Fluid	$R_w/R = 0.95$
" " in a Tunnel	" = 0.96
Observed in Tunnel	" = 0.83

While the tunnel walls inhibit slipstream contraction slightly, this influence is negligible in comparison with the influence of vortex roll-up, and is therefore not considered further.

B. Ultimate Wake Pitch Determined from Actuator Disc Theory

While the actuator disc does not provide a suitable estimate of ultimate wake radius due to vortex roll-up, it can provide an extremely simple estimate of the pitch. We can consider the actuator disc to be represented by a tube of ring vortices proceeding downstream from the plane of the disc. It can be shown from energy considerations that this vorticity must be convected at the average of the slipstream velocity and the free-stream velocity.

If we assume that this convection velocity is the same for a propeller with a finite number of blades operating at an advance coefficient, J, we obtain the simple expression for the pitch of the ultimate wake

$$\frac{P_w}{D} = J\left(\frac{1 + \sqrt{1 + C_T}}{2}\right) . \qquad (9)$$

This expression becomes indeterminate at $J = 0$. However, if we express propeller loading in terms of K_T rather than C_T, we obtain the limit of (9) at static thrust

$$\frac{P_w}{D} = \sqrt{\frac{2K_T}{\pi}} \quad , \qquad J \to 0 \; . \tag{10}$$

V. RESULTS

A summary of measured and calculated results for the DTNSRCD three-bladed propeller series is given in Table 8. Two advance coefficients were considered; the design value of $J = 0.833$, and a lower value of 0.6. The latter results in a thrust coefficient, C_T, of about three times the design value.

At the low advance coefficient, the simple actuator disc formula (10) predicts values of the ultimate wake pitch which are about 89 percent of the measured values, corrected to open water. The pitch predicted from equilibrium of the ultimate wake (8) overestimates the measured value of around three percent for an assumed core radius of 1/50 of the propeller radius.

The sensitivity of the calculated result to core radius is seen to be very weak. An assumed core radius of 1/10 decreases the predicted pitch by three percent, thus coinciding almost exactly with the measured value. However, one can find no physical justification for such a large core radius, except for the possible argument that this allows for the lack of complete roll up of the initial vortex sheet into the core.

At the design advance coefficient, the actuator disc formula again under predicts the pitch, although the results are about 95 percent of the measured values. The pitch predicted from the ultimate wake model is again slightly high.

The results for the stock motorboat propeller are given in Table 9. The trends are remarkably similar to those of Table 8, with the actuator disc approximation slightly under-predicting the measured pitch, and the ultimate wake model

slightly over-predicting its value. The fact that reasonable results are obtained at high values of the propeller thrust coefficient is encouraging.

Open Water J = 0.6, Tunnel J = 0.648 $\pi\lambda_i$ = .960	MODEL NUMBERS			
	4118	4132	4133	4143
Measured C_T in Tunnel	1.82	1.60	2.09	1.67
Measured Pw/D in Tunnel	.850	.828	.870	.791
Measured Pw/D - corrected to open water	.918	.894	.940	.854
Calculated Pw/D - Actuator Disc	.804	.784	.828	.790
Calculated Pw/D - Ultimate Wake r_c = 1/50	.949			
Calculated Pw/D - r_c = 1/25	.933			
Calculated Pw/D - r_c = 1/10	.912			

Open Water J = 0.833 (DESIGN) Tunnel J = 0.862 $\pi\lambda_i$ = 1.041	MODEL NUMBERS			
	4118	4132	4133	4143
Measured C_T in Tunnel	.576	.561	.606	.495
Measured Pw/D in Tunnel	.958	.963	.960	.933
Measured Pw/D - corrected to open water	.991	.996	.993	.965
Calculated Pw/D - Actuator Disc	.939	.937	.944	.926
Calculated Pw/D - Ultimate Wake r_c = 1/50	1.029			
Calculated Pw/D - r_c = 1/25	1.019			
Calculated Pw/D - r_c = 1/10	1.006			

Table 8. Summary of measured and calculated results for DTNSRDC 3-blade propeller series.

	OPEN WATER J			
	.348	.438	.544	.577
Measured C_T in Tunnel	3.650	1.815	.824	.640
Measured Pw/D in Tunnel	.558	.584	.655	.651
Measured Pw/D - corrected to open water	.632	.633	.685	.673
Calculated Pw/D - Actuator Disc	.549	.587	.639	.658
Lifting Line $\pi\lambda_i$	.625	.651	.687	.701
Calculated Pw/D - Ultimate Wake r_c = 1/10	.666			
Measured r_w/R	.821	.803	.803	.830

Table 9. Summary of measured and calculated results for 12 × 8 stock propeller.

VI. APPLICATION TO PROPELLER LIFTING-SURFACE DESIGN

The propeller blade section design computer program designated MIT-PBD-9 [7] was written with the provision for modification of the trajectory of the wake vortices. The wake model developed in the present work has been incorporated in a version of this program designated PDB-A.

The transition wake is defined by a set of discrete vortices originating at each grid point on the trailing edge proceeding to specified hub and tip "roll-up points". The radius, as a function of angular position, is simply assumed to be two parabolic segments with zero slope both at the trailing edge and at the roll-up point. The pitch of each element is uniquely determined from the differences in angular and axial coordinates of the trailing edge starting point and the roll-up point.

Downstream of the roll-up point, the system of discrete vortices degenerates to a single helical vortex from each blade, and an axial hub vortex. This, of course, is simpler from a computational point of view than the usual numerical representation of a complete helical vortex sheet.

A hypothetical propeller with a blade outline identical to 4118, but with a design of J of 0.6 and a design C_T of 1.816 was designed using both PBD-9 and PBD-A, and the results are given in Table 10.

r/R	PITCH RATIO P/D		CAMBER RATIO fo/c	
	βi WAKE (PBD - 9)	DEFORMED WAKE (PBD-A)	βi WAKE (PBD - 9)	DEFORMED WAKE (PBD-A)
.3	.912	.949	.0240	.0259
.5	.990	1.008	.0347	.0348
.7	1.011	1.009	.0345	.0342
.9	.996	.978	.0354	.0352
.95	.996	.976	.0431	.0428

Table 10. Influence of wake deformation on computer pitch and camber

The results labelled "βi WAKE" correspond to a helical wake with a constant pitch/diameter ratio of 0.960 determined by a Lerbs induction factor method lifting-line computer program. The results labelled "DEFORMED WAKE" correspond to a rolled-up wake with a pitch/diameter ratio of 0.849 and a radius of 83% of the propeller radius. The roll-up point was specified to have an axial coordinate of 41% of the propeller radius and an angular coordinate of 90° from the blade tip.

The tabulated results indicate that the influence of wake deformation on blade shape, for a specified circulation distribution, is small. Furthermore, the efficiencies for the two cases computed by integration of forces on the blade in accordance with the procedure outlined in [7] were essentially identical.

This would indicate that there is no particular reason to depart from the classical moderately loaded wake model for the purpose of lifting-surface design computations.

REFERENCES

1. Lap, A. J. W., and van Manen, J. D., "Fundamentals of Ship Resistance and Propulsion", International Shipbuilding Progress, Volume 4, No. 34, June, 1957.

2. Lerbs, H. W., " Moderately Loaded Propellers with Finite Number of Blades and Arbitrary Distribution of Circulation", Trans. SNAME, Volume 60, 1952.

3. Eckhardt, M.K., and Morgan, W.R., "A Propeller Design Method", Trans. SNAME, Volume 63, 1955.

4. Kerwin, J. E., "The Solution of Propeller Lifting-Surface Problems by Vortex Lattic Methods", MIT Department of Naval Architecture Report, 1961.

5. Pien, P. C., "The Calculation of Marine Propellers Based on Lifting-Surface Theory", Journal of Ship Research, Volume 5, No. 2, 1961.

6. Cheng, H. M., "Hydrodynamic Aspects of Propeller Design Based on Lifting-Surface Theory, Parts I and II", David Taylor Model Basin Reports 1802 and 1803, 1964-1965.

7. Kerwin, J. E., "Computer Techniques for Propeller Blade Section Design", International Shipbuilding Progress, Volume 20, No. 227, July, 1973.

8. Kerwin, J. E., and Leopold, R., "A Design Theory for Subcavitating Propellers", Trans. SNAME, Volume 72, 1964.

9. Teel, S., and Denny, S., "Field-Point Pressures in the Vicinty of a Series of Skewed Marine Propellers", Naval Ship Research and Development Center Report 3278, August, 1970.

10. Burrill, L. C., "The Optimum Diameter of Marine Propellers: A New Design Approach," Trans N.E.C.I.E.S., Volume 72, 1955-56.

11. Cummings, D. E., "The Effect of Propeller Wake Deformation on Propeller Design", Third Lips Propeller Symposium, Drunnen, Netherlands, May, 1976.

12. Loukakis, T. A., "A New Theory for the Wake of Marine Propellers", MIT Department of Naval Architecture Report 71-7, May, 1971.

13. Cummings, D. E., "Vortex Interactions in a Propeller Wake", MIT Department of Naval Architecture Report 68-12, June, 1968.

14. Denny, S. B., "Cavitation and Open-Water Performance Tests of a Series of Propellers Designed by Lifting-Surface Methods", Naval Ship Research and Development Center Report 2878, September, 1968.

15. Lamb, H., "Hydrodynamics", Dover Publications, New York.

16. Glauert, H., "Elements of Aerfoil and Airscrew Theory", Cambridge University Press, 1959.

17. Cox, B. D., "Vortex Ring Solutions of Axisymmetric Propeller Flow Problems", MIT Department of Naval Architecture Report 68-13, June, 1968.